Computer Vision- and Human-Robot Interaction-Supported Assembly for Collaborative Off-Earth Habitat Construction

Bier, Henriette; Hidding, Arwin; Prendergast, J.M.; Peternel, Luka

DOI
10.1007/978-981-96-0143-1_9

Publication date
2025

Document Version
Final published version

Published in
Intelligent Computing and Automation

Citation (APA)
Bier, H., Hidding, A., Prendergast, J. M., & Peternel, L. (2025). Computer Vision- and Human-Robot Interaction-Supported Assembly for Collaborative Off-Earth Habitat Construction. In V. Bhateja, M. Dey, & M. Simic (Eds.), *Intelligent Computing and Automation: Proceedings of the 12th International Conference on Frontiers in Intelligent Computing: Theory and Applications (FICTA 2024)* (pp. 103-114). (Smart Innovation, Systems and Technologies; Vol. 421). Springer. https://doi.org/10.1007/978-981-96-0143-1_9

Chapter 9
Computer Vision- and Human-Robot Interaction-Supported Assembly for Collaborative Off-Earth Habitat Construction

Henriette Bier, Arwin Hidding, J. Micah Prendergast, and Luka Peternel

Abstract Rhizome 1.0 and 2.0 are European Space Agency (ESA) co-funded projects that have been implemented with a team from the Architecture, Mechanical Engineering, and Aerospace Engineering Faculties, TU Delft, and various industrial partners. The focus is on the development of a Martian habitat using 3D-printed components and in situ resource utilization. This paper presents a new multi-modal method developed for the collaborative assembly of building components with the support of Computer Vision (CV) and Human-Robot Interaction (HRI) using compliant robotic collaborative manipulators. The building components are Voronoi-based and are fabricated using Design-to-Robotic-Production and -Assembly (D2RP&A). During the collaborative assembly, the robot uses CV to detect the fabricated component and generate autonomous actions to perform the pick-and-place movement. Between the autonomous robot actions, HRI is used by the human to physically guide the robot when grasping and positioning. To evaluate the proposed method, lab experiments were conducted using robotically milled mock-up components from Styrofoam, which were assembled with a collaborative robotic arm. The results indicate that robots can assist humans during the assembly process to implement tasks that are beyond their physical abilities, while robots benefit from human cognitive capabilities during more complex actions.

H. Bier · A. Hidding (✉)
Robotic Building (RB) Lab, Faculty of Architecture and the Built Environment, Delft University of Technology, Julianalaan 134, 2628 Delft, BL, The Netherlands
e-mail: a.j.hidding@tudelft.nl

A. Hidding · J. Micah Prendergast · L. Peternel
Department of Cognitive Robotics (COR), Faculty of Mechanical Engineering, Delft University of Technology, Mekelweg 2, 2628 Delft, CD, The Netherlands

V. Bhateja et al. (eds.), *Intelligent Computing and Automation*, Smart Innovation, Systems and Technologies 421, https://doi.org/10.1007/978-981-96-0143-1_9

9.1 Introduction

Human habitats in off-Earth environments facilitate the implementation of long-term missions. Due to remoteness and constraints on the mission payload, the building process is characterized by the limited availability of tools and workforce, thus multipurpose tools are of the essence.

Collaborative robots are one of the most promising multipurpose tools in space exploration and habitat construction processes. These robots are equipped with various sensors such as Computer Vision (CV) and force sensors that enable Human-Robot Interaction (HRI) to facilitate collaboration during various complex tasks. CV and HRI-supported approaches are not new in the manufacturing industry [2, 21]. The building industry, however, has been slow in picking up the technology [6].

In contrast, the space construction industry relies extensively on this technology, hence, for the ESA-funded projects Rhizome 1.0 and 2.0 a CV- and HRI-supported approach has been explored for assembling 3D-printed components using cement-based and cementless concrete (Fig. 9.1, left) with regolith simulant as aggregate.[1] One of the fundamental tasks in habitat construction is the fabrication [4, 6] and assembly [14] of building components to form the building envelope.

Past works explored the robotic assembly of timber structures where HRI was used to guide the robotic arm haptically during the assembly [8, 20]. More recently, Model Predictive Control (MPC) has been employed to enhance collaborative assembly by incorporating human interaction dynamics and behavior models into the robot control system [9, 18]. Another approach employed HRI for humans to haptically teach the robot how to perform timber assembly after which the robot then executed the assembly autonomously without involving human collaboration [1, 12, 17]. Similarly, autonomous robotic assembly tasks can be taught through teleoperation as opposed to direct physical interaction [15]. Previous work in Rhizome 1.0 [14] involved a collaborative assembly of 3D-printed Voronoi-based components using haptic HRI. While these methods were effective, they involved no vision system thus the robot was heavily dependent on the human to localize the objects and guide the assembly. Other methods used visual feedback in robotic assembly to localize the objects [13, 16]. However, they lacked the HRI element and humans were not incorporated into the assembly process to guide the robot with cognitively and physically complex actions. Recent research [5] combined HRI with CV for the assembly of timber poles into a node. However, that approach lacked the control modalities needed for more complex assembly such as that of 3D-printed Voronoi-based components, which is investigated in this paper.

This paper presents a multi-modal method that combines HRI with CV for the assembly of 3D-printed Voronoi-based components used for the construction of off-Earth habitats. CV detects the component to be picked up by the collaborative robotic arm, based on which a robot end-effector trajectory is generated that moves the robotic

[1] http://www.roboticbuilding.eu/project/rhizome-development-of-an-autarkic-design-to-robotic-production-and-operation-system-for-building-off-earth-habitats/ and http://www.roboticbuilding.eu/project/rhizome-2-0/.

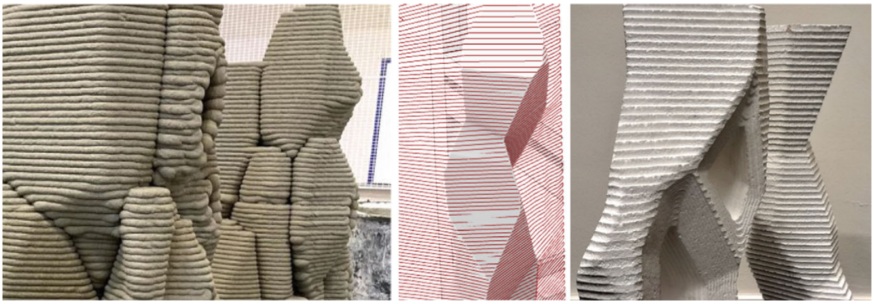

Fig. 9.1 3D-printed Voronoi-based components with regolith simulant as aggregate (left) and mock-up milled components used in CV- and HRI-supported assembly in this study (middle and right)

hand in the vicinity of the component. At that point, the robot switches into compliant mode and the human assists in the complex grasping operation through HRI. The robotic arm then moves the grasped component in the vicinity of the wall where it should be assembled with another component. Finally, the robot mode is switched to complaint mode again and the human uses HRI to complete the assembly process.

9.2 Approach and Methodology

For the proof-of-concept study, mock-up components were robotically milled from Styrofoam (Fig. 9.1, middle and right) using Design-to-Robotic-Production and -Assembly (D2RP&A) method described in Sect. 9.2.1. These are part of a larger Design-to-Robotic-Production-Assembly and -Operation (D2RPA&O) framework linking computational design to robotic production, assembly, and operation of buildings [6]. The proposed method is composed of several key algorithms (see Fig. 9.2 for an overview). The D2RP&A process is described in Sect. 9.2.1. The CV algorithm for the detection and localization of components for assembly is based on the RGB camera, which is described in Sect. 9.2.2. Finally, the multi-modal HRI algorithm for collaborative assembly employs a mode-switching system on a robot end-effector impedance controller and is described in Sect. 9.2.3. The robot control algorithm has two modes: AUTO mode for autonomous movements guided by visual feedback from CV, and HRI mode for human-guided movements via physical interaction.

9.2.1 Design-to-Robotic-Production and -Assembly (D2RP&A)

Design-to-Robotic-Production (D2RP) at the Robotic Building lab, TU Delft involved in the development of a Voronoi-based design from macro, i.e., building, to mezzo,

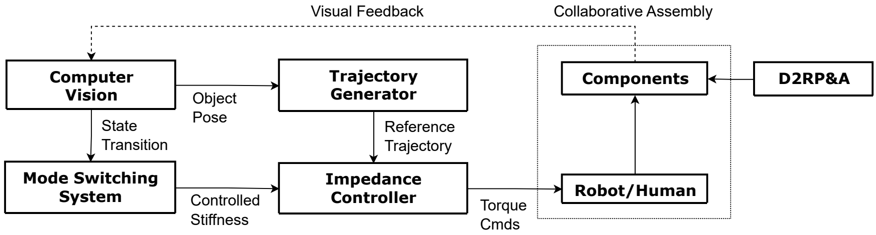

Fig. 9.2 Block scheme of the proposed method. The building components are fabricated using the D2RP&A process. The CV and trajectory generator perform the autonomous robot actions. The mode-switching system enables to switch the robot control mode to HRI where the robot becomes compliant so that human physical guidance can be performed. The low-level control of the robot end-effector is done by an impedance controller

i.e., component, and micro, i.e., material scale. Here is only the mezzo scale presented. Once the to-be-produced components are identified, the milling pre-processing is initiated. The first step is to find the right orientation of the component and create a vacuum-seal mesh for each side, which ensures the milling tool can reach all faces of the component without obstruction. The milling, i.e., tool path, is generated in Grasshopper 3D. The KUKA 6-axis robot has a drilling mill that can drill about 3 cm of foam at a time. The surfaces are milled with patterns mimicking the printing layers, and for the Design-to-Robotic-Assembly (D2RA) task focusing on the CV- and HRI-supported assembly, 2 gripping holes are created (Fig. 9.1).

9.2.2 Computer Vision

Computer Vision (CV) is an important element for working with robots that need to identify and interact with their surroundings. CV allows robots to perceive their environment and localize objects in it. The goal of the CV algorithm is to identify the components, identify where they can be grasped by the robotic arm, and then grasp the components and assemble them. For the CV algorithm, the OpenCV library [7] was employed.

To start the process an image that simulates the conditions the robot will face is created. The image presents the components on a tabletop view (Fig. 9.3). The image is inserted into the CV workflow and processed in a way that returns meaningful inputs for the robot. An edge contour algorithm in this case the Canny edge detector algorithm is run on the image. In this algorithm, a gradient of contrast is used to determine edges. After aligning and calibrating real and virtual images, the pixels of the image are converted into physical units using the frame as a reference object. The image can be used to guide any robot that is connected to the coordinate system of the frame. To identify the edges of the components, they are isolated by using a grayscale contrast threshold implying that any value that is whiter than 240 is made white, and any value darker than 240 is made black allowing easy detection of edges (Fig. 9.3).

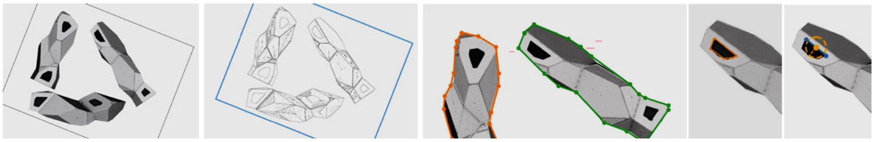

Fig. 9.3 First CV steps involve setting up components on a frame (left) and running a contour-finding algorithm to find external contours (middle left) and components edge detection (middle right), grasping hole edge detection (middle), and grasping vector (right)

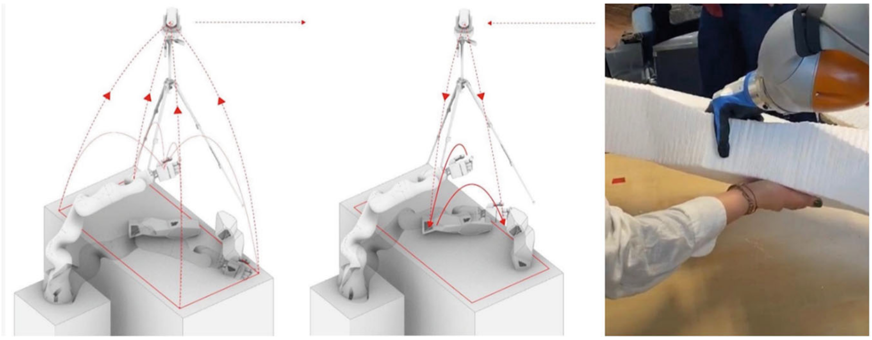

Fig. 9.4 HRI-supported assembly uses robot-to-computer (left) and computer-to-robot (middle) communication relying on a camera to facilitate pick-and-place tasks in collaborating with humans (right)

The next steps are identifying the grasping holes by looking for contours and then creating grasping vectors. This is implemented by creating a vector between 2 points, the contour centroid and the midpoints of the longest edge of the contour. After the components are recognizable for the robot through CV, they are picked and placed, i.e., assembled with HRI support. This is implemented to task the robot with carrying the heavy loads and the human with the precision placing of components where needed and as needed [5].

For the robot to know the exact location of the frame and table, the robotic arm is directed to the vertices of the frame, and these are marked as corresponding vertices in images captured by the camera in the computer. Furthermore, for safety, the robot needs to identify its working area. Therefore, mid-air node points, which direct the moving path of the robotic arm along those points to control its movement are defined (Fig. 9.4). Furthermore, the moving speed is limited to reduce damage in any accidental cases. The robot needs to know the exact and relative position of the components as well. For example, to move a component toward the other component, the hand of the robot would have to grasp the right side to prevent crashing of the arm to the other component. Moreover, the robot should slow down when it is approaching the target component.

9.2.3 Human-Robot Interaction

The goal of the HRI algorithm is to switch between robot modes of operation. In AUTO mode, the robot performs actions autonomously based on the feedback from CV. HRI mode enables humans to physically guide the robotic arm in some of the more complex actions of the task and facilitate collaborative assembly. After the robotic hand reaches the component autonomously based on CV, HRI mode is activated and the human physically guides its hand in terms of how to grasp the component at the grasping hole. This action is relatively complex from both cognitive and physical interaction perspectives as the hand has to be oriented and wiggled into a tight spot. After the component is grasped the trajectory is generated toward the assembly spot and the robot autonomously moves it based on CV. When the moved component is in the vicinity of the assembly location, HRI mode is activated again so that the human can physically guide the hand in orienting and fitting the two components together.

In AUTO mode, the trajectory from the initial pose to the final pose is generated by a quintic polynomial spline function. The final pose is either the vicinity of the object to be grasped or the vicinity of the location where it has to be placed/assembled and is detected by CV. In case CV detects an obstacle in between the movement path, via points can be added to reshape the trajectory and avoid collision.

In HRI mode, the stiffness of the robotic arm is zero so that the robot becomes compliant to the human physical guidance. During AUTO mode where the robot autonomously moves based on the trajectories generated by visual feedback the stiffness of the robotic arm is high, which ensures good tracking precision. The mode-switching system based on robot stiffness control is defined as

$$K = \begin{cases} 0, & \text{if mode} = \text{HRI} \\ \text{high}, & \text{if mode} = \text{AUTO} \end{cases} \tag{9.1}$$

where K is the stiffness modulation term that is used to control the robot end-effector interaction force.

The robotic arm's end-effector force was controlled by the impedance controller [10] as

$$\boldsymbol{F} = \boldsymbol{K}\left(\boldsymbol{x}_{\mathrm{d}} - \boldsymbol{x}_{\mathrm{a}}\right) + \boldsymbol{D}\left(\dot{\boldsymbol{x}}_{\mathrm{d}} - \dot{\boldsymbol{x}}_{\mathrm{a}}\right), \tag{9.2}$$

where $\boldsymbol{F} \in \mathbb{R}^6$ is the end-effector force, $\boldsymbol{x}_{\mathrm{a}} \in \mathbb{R}^6$ is the actual end-effector pose, $\boldsymbol{x}_{\mathrm{d}} \in \mathbb{R}^6$ is the reference end-effector pose. The reference pose is the trajectory generated based on the feedback from the CV algorithm. $\boldsymbol{K} \in \mathbb{R}^{6\times 6}$ and $\boldsymbol{D} \in \mathbb{R}^{6\times 6}$ are the controlled stiffness and damping matrices of the end-effector in Cartesian space. The stiffness was controlled based on the mode-switching system from (9.1). The damping matrix depended on the controlled stiffness and was obtained by double diagonalization design [3].

To produce the designed end-effector force $\boldsymbol{F}$ from (9.2), the robot joint torques were controlled as

$$\boldsymbol{M}(\boldsymbol{q})\ddot{\boldsymbol{q}} + \boldsymbol{C}(\boldsymbol{q}, \dot{\boldsymbol{q}})\dot{\boldsymbol{q}} + \boldsymbol{g}(\boldsymbol{q}) + \boldsymbol{J}^{\mathrm{T}}(\boldsymbol{F} + \boldsymbol{F}_{\mathrm{object}}) = \boldsymbol{\tau}, \tag{9.3}$$

where $\boldsymbol{\tau} \in \mathbb{R}^7$ are the commanded robot joint torques, $\boldsymbol{q} \in \mathbb{R}^7$ are robot joint angles as measured by the encoders, and $\boldsymbol{J} \in \mathbb{R}^{7\times7}$ is the robot Jacobian matrix, $\boldsymbol{M} \in \mathbb{R}^{6\times6}$ is the mass matrix, $\boldsymbol{C} \in \mathbb{R}^{6\times6}$ is the centrifugal and Coriolis matrix and $\boldsymbol{g} \in \mathbb{R}^6$ is the gravity vector. The term $\boldsymbol{F}_{\mathrm{object}} \in \mathbb{R}^6$ is used to compensate for the gravity force of the grasped object, whose weight can be estimated online by the robot force/torque sensors.

To exploit the redundant joints of the robot and enhance the collaboration (e.g., configure itself to not be in the way of the collaborating human), we used null space in the transformation between joint torques and end-effector forces. The augmented joint torque control [11] is given as

$$\boldsymbol{\tau}_{\mathrm{a}} = \boldsymbol{\tau} + \boldsymbol{M}\left(\boldsymbol{I} - \boldsymbol{J}^{\mathrm{T}}\bar{\boldsymbol{J}}^{\mathrm{T}}\right)\boldsymbol{\tau}_{\mathrm{n}}, \tag{9.4}$$

$$\bar{\boldsymbol{J}} = \boldsymbol{M}^{-1}\boldsymbol{J}^{\mathrm{T}}\left(\boldsymbol{J}\boldsymbol{M}^{-1}\boldsymbol{J}^{\mathrm{T}}\right)^{-1}, \tag{9.5}$$

where $\boldsymbol{\tau}_{\mathrm{a}} \in \mathbb{R}^7$ are the commanded robot joint torques augmented with null space joint torques $\boldsymbol{\tau}_{\mathrm{n}}$, and $\bar{\boldsymbol{J}}$ is pseudo-inverse of Jacobian weighted with robot mass matrix $\boldsymbol{M}$. Null space joint torques $\boldsymbol{\tau}_{\mathrm{n}}$ can be then used to control various secondary tasks and they do not interrupt the primary task at the end-effector. For example, a secondary task can be related to the control of the elbow position to be on the other side from where the human is standing and collaborating with the robotic arm so that the robot's structure does not obstruct the human body. In this case, the null space torque is defined as

$$\boldsymbol{\tau}_{\mathrm{n}} = \boldsymbol{J}_{\mathrm{e}}^{\mathrm{T}}\left(\boldsymbol{K}_{\mathrm{e}}(\boldsymbol{x}_{\mathrm{ed}} - \boldsymbol{x}_{\mathrm{ea}}) + \boldsymbol{D}_{\mathrm{e}}(\dot{\boldsymbol{x}}_{\mathrm{ed}} - \dot{\boldsymbol{x}}_{\mathrm{ea}})\right), \tag{9.6}$$

where subscript $_{\mathrm{e}}$ denotes elbow related variables and $\boldsymbol{J}_{\mathrm{e}}$ is Jacobian matrix with end-effector at the elbow.

9.3 Experiments

To validate the proposed method, experiments were conducted on a setup composed of a KUKA LBR iiwa7 collaborative robotic arm equipped with a qb Softhand gripper. For CV, an off-the-shelf RGB camera was mounted above the emulated construction site in the Cognitive Robotics Lab, TU Delft. The communication between all hardware systems was established via Robot Operating System (ROS). Two milled Voronoi-based building components were picked and assembled next to each other. See Fig. 9.5 for the illustration of the experiment setup and task.

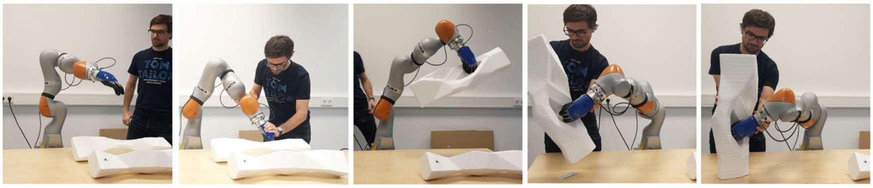

Fig. 9.5 Storyboard composed of photos from the experiment showing the full assembly process involving two components

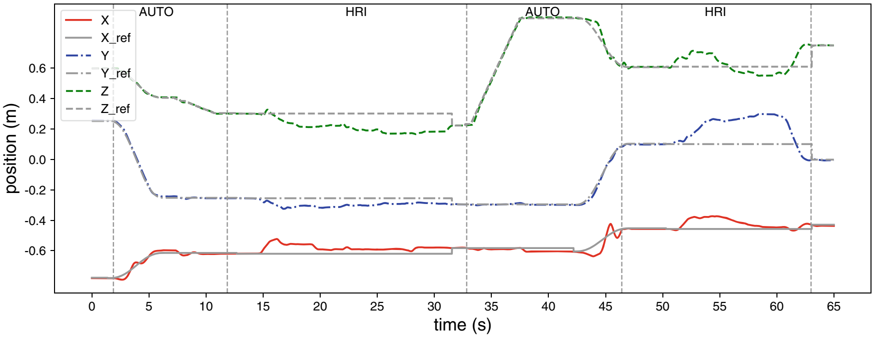

Fig. 9.6 Results of the experiment for the assembly of the second component in a temporal format (left) and in a spatial format (right). In the left graph, the colored lines depict the actual robot end-effector positions, while the gray lines show the reference robot end-effector positions. The robot control modes are indicated at the top with AUTO and HRI and are divided by the vertical dotted gray lines

The experiment task involved moving and assembling two pre-fabricated components at a specific location. Initially, both components were placed on one side of the table lying horizontally. The goal was to assemble them on the other side of the table by placing and attaching them vertically. Figure 9.6 shows the main results of this experiment both in temporal (left) and spatial (right) formats.

The robot started in AUTO mode and had to detect the components and estimate their pose and grasping locations using CV. Next, the robot trajectory planned generated a trajectory that moved its end-effector from its current position into the vicinity of the component. This phase is visible on the graph in Fig. 9.6 (left) between 0 and 12 s. In this mode, the controlled stiffness of the robot end-effector was high and the reference trajectory in the x-axis, y-axis, and z-axis was strictly followed.

When the robot end-effector was in the vicinity of the component grasping location and when the human touched the robot, HRI mode was activated and the robot became compliant. To make the robot compliant, controlled end-effector stiffness was reduced to zero which enabled the human to freely move it through physical interaction. The human then guided the robotic hand to grasp the component. This phase can be seen on the graph in Fig. 9.6 (left) between 12 and 32 s. Since in this mode, the controlled stiffness of the robot end-effector was zero, it can be observed that the reference trajectory in all three axes deviated from the final position of trajectory as the human was doing the fine alignment for the grasping action.

When the component was grasped, the robot control system switched to AUTO mode and generated a trajectory that moved it from the grasped location to the location of the assembly. Since assembly had to be performed in a way that the component was oriented vertically, the robot trajectory also changed the orientation of the grasped component while moving it. This phase is visible on the graph in Fig. 9.6 (left) between 32 and 46 s.

When the robot end-effector was in the vicinity of the assembly location and when the human touched the robot, HRI mode was activated again and the robot became compliant. To make the robot compliant, controlled end-effector stiffness was reduced to zero, which enabled the human to freely move it through physical interaction. The human then guided the robotic hand to grasp the component. This phase is depicted on the graph in Fig. 9.6 between 46 and 62 s. We can see that the reference trajectory in all three axes deviated from the final position of trajectory as the human was doing the fine alignment for the complement placing action.

A supplementary graph in Fig. 9.6 (right) shows the robot end-effector movements spatially in 3D space. The viewpoint is the same as that in Fig. 9.5. When the placement of the first component was completed (green dot on the left), the robot autonomously moved toward the second component, which was at the bottom right section of the graph (blue dot on the right). At this point, the human physically guided the robot during the grasping. After securing the grasp (green dot on the bottom left), the robot autonomously lifted the component and moved it near the assembly location (blue dot on the left). It is visible that the reference trajectory (red) is followed by the actual robot position (gray) in the phases when the robot was in AUTO mode, while it deviated from it during HRI mode when the human was physically guiding the robot hand (Fig. 9.7).

9.4 Discussion

This study presented and evaluated the method that combines CV and HRI for collaborative assembly. The proposed CV- and HRI-supported assembly is targeted for an assembly task that uses non-uniform Voronoi-based components. In this case, robots manufacture the varying polygonal shapes of each component using D2RP methods and pick and place the to-be-expected heavy regolith-based components during the CV- and HRI-supported D2RA phase.

The advantage of this approach is that robots can implement 24/7 tasks faster and more accurately than humans. This implies an increase in the overall productivity of construction processes and reduces the physical workload of humans. In this context, robots and humans are collaborating agents with the robots empowering humans to implement tasks that are beyond their physical abilities thus contributing to flattening hierarchies, i.e., reshaping traditional hierarchical structures, leading to more agile, collaborative, and efficient organizational frameworks and making work

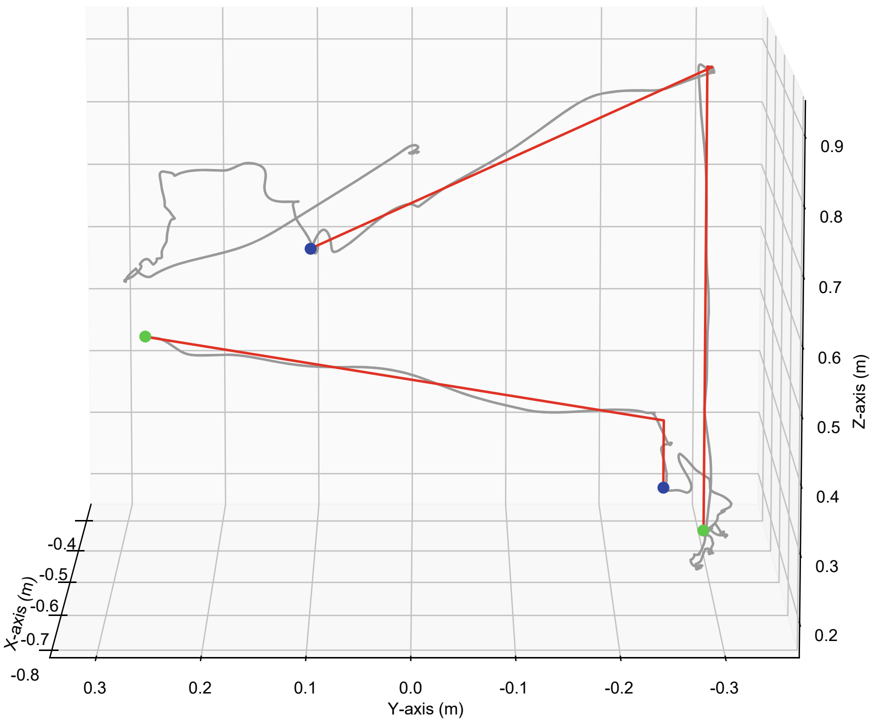

Fig. 9.7 Results of the experiment for the assembly of the second component in a spatial format. The red line depicts the actual robot end-effector positions, while the gray line shows the reference robot end-effector positions. Green dots indicate the beginnings of the autonomous robot movements, while blue dots indicate their ends

environments more inclusive and accessible for women and disabled individuals. On the other hand, the approach retains human involvement and utilizes superior human cognitive capabilities to guide the robot during more complex actions.

Considering that CV relies on detecting the outline of the components in the Martian environment that is dusty and lacks light, possibly blurring the vision and obstructing the computer from detecting the object's outline additional measures have to be taken. Also, inaccuracy occurring during the conversion of 3D images into 2D data requires improvements in Python script for more accurate outline-detection using convolution, and 3D scanning, which can be incorporated for the future use of the presented approach.

A potential improvement to the AUTO part is to upgrade the trajectory generation algorithm. In this study, a spline method that can generate a smooth trajectory between the given via-points was used. While this is effective for autonomous actions, it is difficult for humans to directly adapt/teach the trajectories via physical interaction by using the spline method. For that purpose, a better approach would be to use a method such as Dynamic Movement Primitives (DMPs) [19] where humans can adapt/teach the trajectories online through physical interaction.

Acknowledgements This paper has profited from the contribution of TU Delft students, in particular C. Bianco, D. Sauer, M. Waszkiewicz, and Sit Chi Man (Simon) under the supervision of experts from Robotic Building, AiDAPT, and Cognitive Robotics Labs at TU Delft.

References

1. Abu-Dakka, F.J., Nemec, B., Kramberger, A., Buch, A.G., Krüger, N., Ude, A.: Solving peg-in-hole tasks by human demonstration and exception strategies. Ind. Robot Int. J. **41**(6), 575–584 (2014)
2. Ajoudani, A., Zanchettin, A.M., Ivaldi, S., Albu-Schäffer, A., Kosuge, K., Khatib, O.: Progress and prospects of the human-robot collaboration. Auton. Robots **42**, 957–975 (2018)
3. Albu-Schaffer, A., Ott, C., Frese, U., Hirzinger, G.: Cartesian impedance control of redundant robots: recent results with the DLR-light-weight-arms. In: 2003 IEEE International Conference on Robotics and Automation (ICRA), pp. 3704–3709. IEEE (2003)
4. Bier, H., Hidding, A., Latour, M., Oskam, P., Alavi, H., Külekci, A.: Design-to-robotic-production and-operation for activating bio-cyber-physical environments. In: Disruptive Technologies: The Convergence of New Paradigms in Architecture, pp. 45–57. Springer (2023)
5. Bier, H., Khademi, S., van Engelenburg, C., Prendergast, J.M., Peternel, L.: Computer vision and human-robot collaboration supported design-to-robotic-assembly. Constr. Robot. **6**(3–4), 251–257 (2022)
6. Bier, H., Liu Cheng, A., Mostafavi, S., Anton, A., Bodea, S.: Robotic building as integration of design-to-robotic-production and-operation. In: Robotic Building, pp. 97–120 (2018)
7. Bradski, G.: The OpenCV library. Dr. Dobb's J. Softw. Tools Prof. Program. **25**(11), 120–123 (2000)
8. Devadass, P., Stumm, S., Brell-Cokcan, S.: Adaptive haptically informed assembly with mobile robots in unstructured environments. In: Proceedings of the 36th International Symposium on Automation and Robotics in Construction (ISARC), vol. 36, pp. 469–476 (2019)
9. Haninger, K., Hegeler, C., Peternel, L.: Model predictive impedance control with Gaussian processes for human and environment interaction. Robot. Auton. Syst. **165**, 104431 (2023)
10. Hogan, N.: Impedance control: an approach to manipulation: part II—implementation. J. Dyn. Syst. Meas. Control **107**(1), 8–16 (1985)
11. Khatib, O.: A unified approach for motion and force control of robot manipulators: the operational space formulation. IEEE J. Robot. Autom. **3**(1), 43–53 (1987)
12. Kramberger, A., Kunic, A., Iturrate, I., Sloth, C., Naboni, R., Schlette, C.: Robotic assembly of timber structures in a human-robot collaboration setup. Front. Robot. AI **8**, 768038 (2022)
13. Kunic, A., Naboni, R., Kramberger, A., Schlette, C.: Design and assembly automation of the robotic reversible timber beam. Autom. Constr. **123**, 103531 (2021)
14. Loopik, H., Peternel, L.: A multi-modal control method for a collaborative human-robot building task in off-earth habitat construction. In: Workshop on Design, Learning, and Control for Safe Human-Robot Collaboration (ICAR 2021) (2021)
15. Peternel, L., Petrič, T., Babič, J.: Robotic assembly solution by human-in-the-loop teaching method based on real-time stiffness modulation. Auton. Robots **42**, 1–17 (2018)
16. Rogeau, N., Tiberghien, V., Latteur, P., Weinand, Y.: Robotic insertion of timber joints using visual detection of fiducial markers. In: Proceedings of the 37th International Symposium on Automation and Robotics in Construction (ISARC), pp. 491–498 (2020)
17. Roveda, L., Magni, M., Cantoni, M., Piga, D., Bucca, G.: Human-robot collaboration in sensorless assembly task learning enhanced by uncertainties adaptation via Bayesian optimization. Robot. Auton. Syst. **136**, 103711 (2021)
18. Roveda, L., Testa, A., Shahid, A.A., Braghin, F., Piga, D.: Q-learning-based model predictive variable impedance control for physical human-robot collaboration. Artif. Intell. **312**, 103771 (2022)

19. Saveriano, M., Abu-Dakka, F.J., Kramberger, A., Peternel, L.: Dynamic movement primitives in robotics: a tutorial survey. Int. J. Robot. Res. **42**(13), 1133–1184 (2023)
20. Stumm, S., Devadass, P., Brell-Cokcan, S.: Haptic programming in construction: intuitive on-site robotics. Constr. Robot. **2**, 3–13 (2018)
21. Zhou, L., Zhang, L., Konz, N.: Computer vision techniques in manufacturing. IEEE Trans. Syst. Man Cybern. Syst. **53**(1), 105–117 (2022)